Journal of Biomaterials Applications

TiO$_2$-doped phosphate glass microcarriers: A stable bioactive substrate for expansion of adherent mammalian cells

Joana C Guedes, Jeong-Hui Park, Nilay J Lakhkar, Hae-Won Kim, Jonathan C Knowles and Ivan B Wall

The online version of this article can be found at:
http://jba.sagepub.com/content/28/1/3

Published by:
$SAGE

http://www.sagepublications.com

Additional services and information for *Journal of Biomaterials Applications* can be found at:

Open Access: Immediate free access via SAGE Choice

Email Alerts: http://jba.sagepub.com/cgi/alerts

Subscriptions: http://jba.sagepub.com/subscriptions

Reprints: http://www.sagepub.com/journalsReprints.nav

Permissions: http://www.sagepub.com/journalsPermissions.nav

Citations: http://jba.sagepub.com/content/28/1/3.refs.html

>> Version of Record - Jun 28, 2013

OnlineFirst Version of Record - Aug 30, 2012

What is This?

TiO₂-doped phosphate glass microcarriers: A stable bioactive substrate for expansion of adherent mammalian cells

Joana C Guedes[1,2], Jeong-Hui Park[3,4], Nilay J Lakhkar[5], Hae-Won Kim[3,4], Jonathan C Knowles[4,5] and Ivan B Wall[1,4]

Abstract
Scalable expansion of cells for regenerative cell therapy or to produce large quantities for high-throughput screening remains a challenge for bioprocess engineers. Laboratory scale cell expansion using t-flasks requires frequent passaging that exposes cells to many poorly defined bioprocess forces that can cause damage or alter their phenotype. Microcarriers offer a potential solution to scalable production, lending themselves to cell culture processes more akin to fermentation, removing the need for frequent passaging throughout the expansion period. One main problem with microcarrier expansion, however, is the difficulty in harvesting cells at the end of the process. Therefore, therapies that rely on cell delivery using biomaterial scaffolds could benefit from a microcarrier expansion system whereby the cells and microcarriers are transplanted together. In the current study, we used bioactive glass microcarriers doped with 5% TiO₂ that display a controlled rate of degradation and conducted experiments to assess biocompatibility and growth of primary fibroblast cells as a model for cell therapy products. We found that the microcarriers are highly biocompatible and facilitate cell growth in a gradual controlled manner. Therefore, even without additional biofunctionalization methods, Ti-doped bioactive glass microcarriers offer potential as a cell expansion platform.

Keywords
Microcarriers, bioactive phosphate-based glass, cell expansion, titanium

Introduction

The emerging field of regenerative medicine incorporates strategies including cell therapy, biomaterial scaffolds and small molecules to stimulate regeneration in the body. In particular, direct cell delivery or tissue engineering approaches have the aim of restoring function of injured or diseased body parts by delivery of cells or engineered tissues to the defect site.[1] This promising strategy depends on the assumption that cells can be expanded to produce therapeutic quantities and then be differentiated into the appropriate cell type required in the defect site.

Current limitations to cell therapy include expanding cells to the desired number for clinical use and the fact that their extended expansion in culture leads to loss of multipotency and senescence.[2] For example, bioprocess forces experienced during serial passaging of cells (including centrifugal, hydrodynamic and capillary flow shear stress) can have poorly defined and, indeed, undesired effects on the cells. Moreover, interactions of adhesion molecules with extracellular matrix (ECM) ligands required to support cell survival are cyclically interrupted by trypsinization and

[1]Department of Biochemical Engineering, University College London, Torrington Place, London, UK
[2]Department of Bioengineering, Insituto Superior Técnico, Avenida Rovisco Pais, Lisboa, Portugal
[3]Institute of Tissue Regeneration Engineering (ITREN), Dankook University, Cheonan, Republic of Korea
[4]Department of Nanobiomedical Science and WCU Research Center, Dankook University, Cheonan, Republic of Korea
[5]Division of Biomaterials and Tissue Engineering, UCL Eastman Dental Institute, University College London, London, UK

Corresponding author:
Ivan B Wall, Department of Biochemical Engineering, University College London, Torrington Place, London WC1E 7JE, UK.
Email: i.wall@ucl.ac.uk

replating during every passage in 2-dimensional (2D) monolayer expansion.[3] Therefore, reliable and efficient *ex vivo* cell expansion methods need to be explored as alternatives to conventional 2D culture systems. Microcarriers that offer large surface areas for growth of anchorage-dependent cells have a potential advantage in that they can be used for the expansion of adherent cells in a 3D bioreactor using processes that are more akin to fermentation processes than traditional 2D monolayer cell culture. In recent years, several methods of expanding adherent cells have been reported using different types of microcarriers as substrates for cell attachment.[4,5] Bead size, surface area and functional ability to promote cell attachment are all critical factors that can affect cell adhesion and ultimately their expansion potential.[6]

Recent advances in the biomaterials field have led to the development of composite materials, biofunctionalized to complement and enhance biological responses in living tissues without compromising the natural biological process. These materials include glasses and glass-ceramics and can be considered as bioactive materials.[7] One of the measures of bioactivity is the utilization of simulated body fluid (SBF) in which apatite formed on the surface of a material is taken as an indicator that the material is bioactive.[8] Phosphate-based glasses are particularly attractive as they are easy to produce, biodegradable and of known biocompatibility with multiple cell types.[9,10] They can also be doped with a variety of metal oxides to modify their physical properties or induce a specific function such as antimicrobial capacity.[11] However, they have been shown to not form an apatite layer *in vitro*,[12] and yet do upregulate genes associated with bone formation in cell culture.[13]

The potential of microcarriers made of such materials for tissue engineering is significant because they present a potential way in which large quantities of material could be produced in many small individual cell-microcarrier units that can then be pieced together after expansion is accomplished.

In the current study, we selected microcarriers made from a stable bioactive phosphate glass doped with 5 mol% TiO_2 to assess the attachment and expansion of primary fibroblasts as a model system for somatic cells used in cell therapy and tissue engineering procedures.

Materials and methods

Glass preparation and microsphere formation

Glasses were synthesized from the precursors: sodium dihydrogen orthophosphate (NaH_2PO_4), calcium carbonate ($CaCO_3$), phosphorous pentoxide (P_2O_5) and titanium dioxide (TiO_2) as previously described.[14]

Table 1. Glass structural composition.

Glass codes	Glass compositions (mol%)			
	P_2O_5	CaO	Na_2O	TiO_2
P50C40N7Ti3 (Ti3)	50	40	7	3
P50C40N5Ti5 (Ti5)	50	40	5	5
P50C40N3Ti7 (Ti7)	50	40	3	7

Three different compositions, Ti3, Ti5 and Ti7 were made, according to the TiO_2 content used (Table 1). The precursors were weighed and mixed and then pre-heated to 700°C for 30 min to remove CO_2 and H_2O. The mixture was then melted at 1300°C for 3 h and then rapidly quenched onto a steel plate. The phosphate glasses were ball-milled and sieved down to 75–106 μm. The glass particles were then passed through a flame spheroidization device to produce microspheres as previously described.[12] The size distribution of the resulting microspheres was 10–210 μm and a size range of 63–106 μm was selected for use in subsequent experiments.

Characterization of dissolution and ion release

To determine the change in weight with time, 250 mg of microspheres were placed in 25 ml of deionised water at pH 7. At 0, 1, 3, 7, 14 and 21 days, the solution was removed and the samples were oven dried and then reweighed and the weight loss was calculated as a percentage of the original weight. A unique set of samples was prepared for each time point and each time point was measured in triplicate.

ICS-1000 ion chromatography system (Dionex, UK) was used to measure Na^+ and Ca^{2+} release. The separation was performed using methanesulfonic acid (Fluka, UK) eluent and a 4×250 mm Ion Pac® CS12A separator column. Prior to running a sample, ion chromatograph was calibrated against a four-point calibration curve using a predefined calibration routine. The Chromeleon® software package was used for data analysis.

The phosphate anion measurements were carried out using a Dionex ICS-2500 ion chromatography system. Polyphosphates were eluted using a 4×250 mm Ion Pac® AS16 anion-exchange column packed with anion exchange resin. A Dionex anion self-regenerating suppressor (ASRS®) was used at 242 mA. The Dionex EC40 eluent generator equipped with a potassium hydroxide (KOH) cartridge was used in conjunction with the ASRS®. The sample run time was set for 20 min where the gradient program started from 30 mM KOH for 10 min, then increased from 30 to 60 mM KOH over 5 min, followed by remaining at

60 mM KOH for 3 min and finally the KOH returned to 30 mM for 2 min.

Average microcarrier diameter measurements

Average microcarrier diameter was determined from light micrograph images of microcarrier monolayers. The diameter of 200 microcarriers was measured using the Image J software. Frequency histograms of size distribution were created in order to determine the size range of microcarriers employed.

Isolation and culture of primary fibroblasts

Primary fibroblasts were derived from E12.5-13.5 CD-1 mouse embryos in accordance with local animal welfare guidelines and regulations. Fibroblasts were liberated from embryonic tissue using the collagenase digestion method described previously.[15] Cultures were established by plating digested tissue in T-25 flasks and cultured with Dulbecco's Modified Eagle Medium (DMEM) (4.5 g/L glucose) supplemented with FBS (10%) and non-essential amino acids (1%) (all from Invitrogen, Paisley, UK). Cell cultures were maintained at $37^{\circ}C/5\% CO_2$ and passaged when 80-90% confluent using trypsin-EDTA solution for 3 min at $37^{\circ}C$. Cell number was quantified using a Neubauer haemocytometer and viability was determined using the Trypan blue dye exclusion method.

Relative attachment of primary fibroblasts to microcarriers versus cell culture-grade plastic. Bioactive glass microcarriers (15 mg/well) were placed into wells of a 96-well microwell plate (Greiner Bio-One, Stonehouse, UK) in a monolayer and UV sterilized for 1 h and 40 min. Microcarriers were then equilibrated in 50 µL of pre-warmed medium to 'wet' them and avoid putting the cell suspension directly onto a dry monolayer of microcarriers. Fibroblasts were seeded on microcarriers (1.5×10^4 cells in 50 µL of medium) and the plates were then incubated at $37^{\circ}C$ and $5\% CO_2$ for 24 h. Observations of cell attachment to microcarriers compared to the surrounding cell culture plastic were made using light microscopy and subsequently using fluorescence microscopy after staining with DAPI.

Primary fibroblast expansion on microcarriers in low-adhesion microwell plates

Low attachment 96-well plates (Costar®) were used for cell proliferation studies to prevent undesired cell attachment to the microwell surface. After sterilizing as above, microcarriers were equilibrated in 50 µL of pre-warmed medium. Fibroblasts in 50 µL of medium were then seeded onto microcarriers at a concentration of 1.5×10^4 cells/well and the plates were incubated at $37^{\circ}C/5\% CO_2$ for different time periods of up to 14 days. Medium was replaced every 48 h.

Cell staining procedures

Live cell staining was performed by incubating a confluent T-25 flask of fibroblasts with staining solution consisting of 10 µL Vybrant DiO labeling dye (Invitrogen) in 2 mL of normal growth medium at $37^{\circ}C$ for 20 min. Staining medium was removed and cells washed three times with PBS.

4′, 6-diamidino-2-phenylindole (DAPI) staining was performed after fixing cells with 4% paraformaldehyde (PFA) for 10 min at room temperature (RT) and washing with PBS. Cultures were stained with DAPI (working solution 1:1000) for 5 min at $37^{\circ}C$ and then rinsed with PBS.

For actin cytoskeleton labeling, cells were fixed with 4% PFA for 10 min at RT and then permeabilized with 0.5% Triton X-100 in PBS for 5 min at RT. Cultures were stained with Acti-stain™ 488 phalloidin (1:140 dilution in PBS) (Cytoskeleton, Inc.) for 30 min at RT in the dark. Counter-staining with propidium iodide (PI) was performed by fixing cells as above, then permeabilizing with 0.1% Triton X-100 in PBS for 5 min at RT. Cells were stained with PI (10 µg/mL; Sigma) for 5 min at RT in the dark.

PI and phalloidin labeling were visualized by confocal microsopy using a Radiance 2100 confocal microscope (BioRad, Loughborough, UK).

Cell proliferation assays

Cell proliferation was measured the Cell Counting Kit-8 (CCK-8; Sigma). Fibroblasts were seeded onto monolayers of bioactive glass microcarriers (15 mg/well) in 96-well low adhesion microwell plates at a concentration of 1.5×10^4 cells/well and incubated at $37^{\circ}C$. At different time points up to 14 days, optical density was measured at 450 nm in a multi-well Safire2 plate reader (Tecan). Cells cultured in 96-well tissue culture grade plates were used as a positive control due to their capacity to enhance cell proliferation. All samples were assayed in triplicate and for each experiment the mean ± standard deviation was calculated.

Scanning electron microscopy

For scanning electron microscopy (SEM), fibroblasts (3×10^4 cells/well) were seeded onto bioactive glass microcarriers (40 mg/well) in 24-well plate tissue culture inserts (Greiner Bio-One, Stonehouse, UK). After culture for 1, 3 or 7 days, cells on microcarriers were prepared SEM using established protocols.[16] Briefly, cells were fixed (3% glutaraldehyde in 0.1 M cacodylate

buffer for 24 h at 4°C), dehydrated, critical-point dried using hexamethyldisilazane, air-dried and then mounted onto aluminium pin stubs and coated with gold/palladium. Samples were examined with a JEOL 5410LV SEM (JEOL UK) operating at 10 kV.

Results

Microcarrier dissolution and ion release

Microcarriers doped with three different concentrations of TiO_2 were subjected to dissolution studies to determine their stability. Figure 1(A) shows the weight change over time for beads containing 3, 5 and 7 mol% TiO_2. As expected, the glass with the lowest TiO_2 content showed the highest degradation rate and is relatively linear with time. The glasses containing 5 and 7 mol% TiO_2 however appeared to be more stable and showed very similar patterns of degradation behavior, with an initial drop in weight up to day 3 and overall losing around 15% of their total weight at 21 days. Ca^{2+} release data also confirmed this (Figure 1(B)), with the lowest TiO_2 content glass releasing Ca^{2+} at a greater rate due to rapid degradation. The glasses with 5 and 7 mol% TiO_2 showed relatively similar Ca^{2+} release profiles, with the glass containing 5 mol% TiO_2 having a slightly higher Ca^{2+} release profile. All three glasses showed relatively linear Ca^{2+} release with time. The ionic release of other ionic species is shown in Table 2. The release rates were calculated from the respective graphs of ion release with time, whereby a straight line was fitted through the data, passing through the origin. All the other ions showed a similar release pattern to the Ca^{2+} (data not shown), differing only in the rates at which the ions were released. The Ti^{4+} was not measured due to the very low levels released, making the measurements unreliable. Due to the relatively similar stability of Ti5 and Ti7, we used Ti5 microcarriers for subsequent experiments using fibroblasts. The mean microcarrier diameter of the Ti5 batch was $84.2 + 19.4\,\mu m$ and approximately 1450 microcarriers were required to cover the surface of one well of a 96-well microplate. Microscopic appearance and size distribution of a sample of 200 microcarriers are shown in Figure 1(C) and (D).
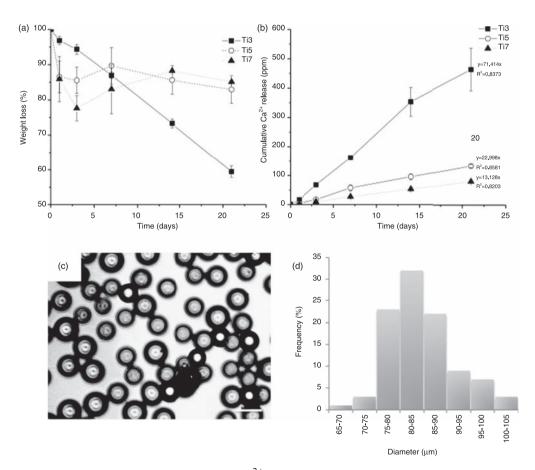

Figure 1. (A) Microcarrier degradation and (B) associated Ca^{2+} release from Ti3, Ti5 and Ti7 microcarriers over time in deionized water. (C) Light micrograph of microscopic appearance and (D) size distribution histogram of Ti5 microcarriers used in subsequent experiments. Bar = 100 μm.

Microscopic characterization and fibroblastic cell affinity of TiO₂-doped microcarriers. Examinations of cell attachment to 5 mol% TiO₂ glass microcarriers was conducted initially in standard cell culture plates to determine whether cells can attach to the microcarrier surface or instead show preference for the highly permissive cell culture grade plastic surface. We observed that even though many fibroblasts were established on the tissue culture plastic by 24 h, fibroblasts could readily adhere to the microcarrier surfaces where they came into contact with them (Figure 2(A) and (B)). Having confirmed that the microcarriers are not inhibitory to cell growth when placed in competition with tissue culture plastic, fibroblasts were then seeded onto microcarriers in low-adhesion microwell plates and after 72 h all cells attached to the microcarriers and not the bottom of the microwell (Figure 2(C)–(E)). Morphology

was assessed in greater detail on 5 mol% TiO₂-doped microcarriers after 3 days of culture (Figure 3). Labeling of the actin cytoskeleton (green) revealed that fibroblasts wrap themselves around the microcarrier and prominent focal adhesion sites are evident (arrows). Cell nuclei staining also revealed cells actively dividing on the microcarrier surface (arrowheads).

Fibroblast proliferation capacity on microcarrier surfaces

Proliferation of primary fibroblasts on TiO₂-doped microcarriers in low-adhesion microwell plates was assayed under static conditions and compared to routine cell culture-grade microwell plates that provide optimal substrate properties to enhance cell expansion. The CCK proliferation assay revealed that a steady, sustained expansion of the population was achievable over 14 days of culture for 2 different passages of cells tested, culminating in a 2-fold increase in the population size after 14 days ($p < 0.01$) (Figure 4). However, proliferation was only 50% of that in routine cell culture grade microwell plates.

Interconnectivity and network forming capacity of fibroblast-microcarrier cultures. Fibroblasts are able not only to adhere to microcarriers but also readily form 3D networks in static culture as soon as 24 h after seeding by bridging across to adjacent microcarriers and to cells located on adjacent microcarriers
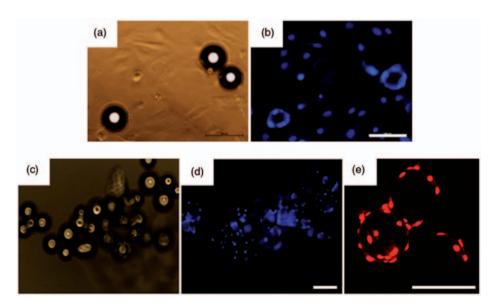
Table 2. Release rate of ionic constituents from microcarriers.

Glass code	Ti3	Ti5	Ti7
Anion (ppm h⁻¹)			
PO_4^{3-}	37.921	5.2563	3.6023
$P_3O_9^{3-}$	46.864	13.304	7.4739
$P_2O_7^{4-}$	15.084	3.2237	2.2045
$P_3O_{10}^{5-}$	18.761	8.1531	5.5788
Cation (ppm h⁻¹)			
Ca^{2+}	45.778	15.202	7.462
Na^+	15.571	1.9666	0.772

Figure 2. (A) Phase-contrast and (B) DAPI staining of fibroblasts seeded onto standard tissue culture plastic dispersed with microcarriers after 24 h. (C–D) Adhesion of fibroblasts to microcarriers in ultra-low attachment microwell plates 72 h after seeding. (E) Clear cell adhesion and growth on microcarriers is evident with propidium iodide (PI) staining at high power after 72 h. Bar = 100 μm.
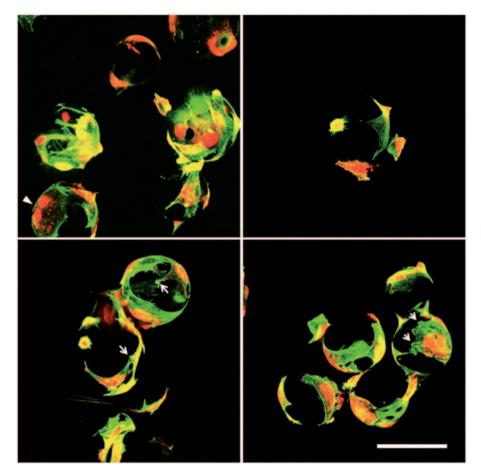
Figure 3. Morphology of fibroblasts cultured on 5 mol% TiO$_2$-doped microcarriers. Green = phalloidin f-actin; Red = propidium iodide; arrows = focal adhesions; arrowhead = dividing cell. Bar = 100 μm.
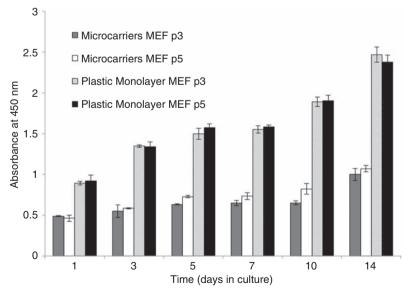

Figure 4. Proliferation of fibroblasts cultured on 5 mol% TiO$_2$-doped microcarriers and on standard tissue culture plastic. Values = mean ± standard deviation.
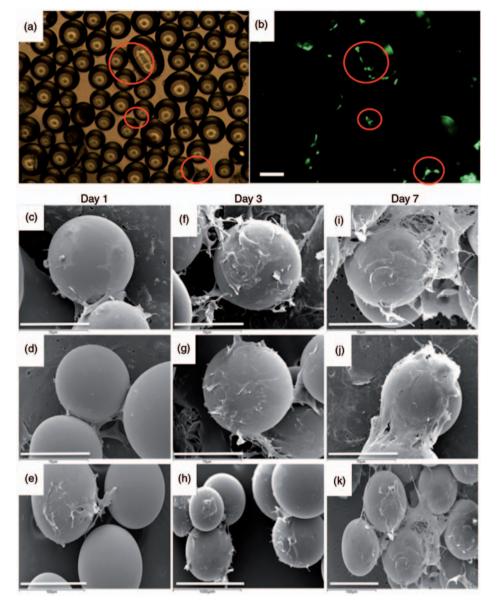
Figure 5. (A) Phase contrast and (B) fluorescent images of fibroblasts labelled with Vibrant DiO after 24 h. (C–K) Scanning electron microscopy (SEM) images showing morphology of fibroblasts over time. Bar A, B, E, H, K = 100 μm; C, D, F, G, I, J = 70 μm.

(Figure 5(A) and (B)). SEM reveals this to an even greater extent over a period of 7 days culture and the extensive network of cell processes between microcarriers reveals that a high degree of biocompatibility is evident (Figure 5(C)–(K)) and that the combined fibroblast-microcarrier system was capable of forming a large interconnected 3D network.

Discussion

The degradation rate of phosphate glasses, and consequently their biocompatibility, is mainly dependent on the glass composition; therefore, suitable modifications to the glass chemistry are required in order to obtain

stable substrates that degrade slowly and exhibit high biocompatibility. In the current study, microcarriers were doped with several different concentrations of TiO_2 and while 3 mol% microcarriers were found to degrade too rapidly to be useful for either scalable cell expansion or clinical delivery, the 5 and 7 mol% compositions were structurally stable over the time period examined. There was evidence of more rapid initial degradation in the 5 and 7 mol% glass and this may be due to the rate at which Na^+ is initially released, which may come out of these glasses more quickly. However, the rest of the structure is relatively more stable in solution, hence the reduction in weight loss. The 5 mol% TiO_2-doped microcarriers were used

for subsequent cytocompatibility work using primary fibroblasts and it was found that cell adhesion and proliferation was supported on the microcarriers. This is attributable to the known biocompatibility of TiO_2.[17] Furthermore, after a static culture period of 7 days, cells formed a large amount of bridging between adjacent microcarriers. However, for scalable expansion processes, dynamic bioreactor culture would be employed to ensure homogeneous dispersion of microcarriers and efficient mixing of nutrients. Significant cell bridging between microcarriers after 7 days of culture raises the possibility that they would be suitable for forming dynamic tissue-engineered structures after an initial period of dynamic culture.

A dynamic approach to scalable cell expansion amenable to tissue engineering by producing tissue-engineered microunits would be highly beneficial for tissue regeneration purposes. However, our aim in the current study was to demonstrate the biocompatibility of TiO_2-doped glass microspheres and feasibility of the surface to serve as a suitable surface for cell adhesion and growth. While cell growth was not as rapid as on commercially available tissue culture plastic designed and optimised to enhance cell growth, surface modifications to the TiO_2-doped microcarriers should overcome this concern. Cell culture grade plastic is surface-modified to enhance cell growth and subsequent improvements to the microcarriers such as biofunctionalization of the surface may be a suitable strategy to enhance cell growth. Biofunctionalization methods, such as surface coating with ECM molecules or short peptides that can mimic extracellular or growth factor motifs,[18] have been successful for polymer-based scaffolds of low intrinsic biocompatibility.

Traditional tissue engineering strategies employ a "top-down" approach, in which cells are seeded on a biodegradable scaffold. Using this approach, the cells are expected to populate the scaffold and create the appropriate ECM and microarchitecture. However, it is very difficult to replicate tissue microarchitecture using a top-down approach even in spite of the wealth of advanced surface biofunctionalization methods and native decellularized scaffolds available. In a "bottom-up" approach, modular tissue engineering aims to address the challenge of recreating biomimetic structures by designing structural features on the micron scale to build modular tissues that can be used as building blocks to create larger tissues.[19] The use of TiO_2-doped microcarriers for modular tissue engineering is particularly promising for bone regeneration strategies as titanium is widely used for orthopaedic and dental procedures, supporting osteogenesis even when a disease such as diabetes dampens the intrinsic regeneration response.[20–22]

Compared to pre-fabricated bulk scaffolds, microcarriers offer a range of unique features: (a) expansion capacity that can be scaled according to the individual patient requirements such as size of defect; (b) the possibility of easy and quick injection without larger surgical procedures[23]; (c) enhanced versatility in fitting the unique, site-specific shape of a defect as compared to a pre-fabricated bulk scaffold and (d) homogeneous distribution of cells throughout an agglomerated construct of cell-loaded microcarriers. These features make microcarriers a promising alternative to bulk scaffolds.

Conclusions

TiO_2-doped bioactive glass microcarriers offer great potential as a scalable expansion tool for the cell therapy industry and may also serve a dual purpose by doubling as a dynamic method for tissue engineering. Surface modifications for further biofunctionalization could yield microcarriers that are valuable tools for cell expansion and tissue engineering.

References

1. Langer R and Vacanti JP. Tissue engineering. *Science* 1993; 260: 920–926.
2. Banfi A, Bianchi G, Notaro R, et al. Replicative aging and gene expression in long-term cultures of human bone marrow stromal cells. *Tissue Eng* 2002; 8: 901–910.
3. Reddig PJ and Juliano RL. Clinging to life: cell to matrix adhesion and cell survival. *Cancer Metastasis Rev* 2005; 24: 425–439.
4. Eibes G, dos Santos F, Andrade PZ, et al. Maximizing the ex vivo expansion of human mesenchymal stem cells using a microcarrier-based stirred culture system. *J Biotechnol* 2010; 146: 194–197.
5. Santos F, Andrade PZ, Abecasis MM, et al. Toward a clinical-grade expansion of mesenchymal stem cells from human sources: a microcarrier-based culture system under xeno-free conditions. *Tissue Eng Part C Methods* 2011; 17: 1201–1210.
6. Hammond TG and Hammond JM. Optimized suspension culture: the rotating-wall vessel. *Am J Physiol Renal Physiol* 2001; 281: F12–F25.
7. Kokubo T, Kim HM, Kawashita M, et al. Bioactive metals: preparation and properties. *J Mater Sci Mater Med* 2004; 15: 99–107.
8. Kokubo T and Takadama H. How useful is SBF in predicting *in vivo* bone bioactivity? *Biomaterials* 2006; 27: 2907–2915.

9. Ahmed I, Collins CA, Lewis MP, et al. Processing, characterisation and biocompatibility of iron-phosphate glass fibres for tissue engineering. *Biomaterials* 2004; 25: 3223–3232.

10. Bitar M, Salih V, Mudera V, et al. Soluble phosphate glasses: *in vitro* studies using human cells of hard and soft tissue origin. *Biomaterials* 2004; 25: 2283–2292.

11. Neel EA, Ahmed I, Pratten J, et al. Characterisation of antibacterial copper releasing degradable phosphate glass fibres. *Biomaterials* 2005; 26: 2247–2254.

12. Lakhkar NJ, Park JH, Mordan NJ, et al. Titanium phosphate glass microspheres for bone tissue engineering. *Acta Biomater* 2012. http://dx.doi.org/10.1016/j.actbio.2012.07.023.

13. Abou Neel EA, Mizoguchi T, Ito M, et al. *In vitro* bioactivity and gene expression by cells cultured on titanium dioxide doped phosphate-based glasses. *Biomaterials* 2007; 28: 2967–2977.

14. Abou Neel EA, Chrzanowski W and Knowles JC. Effect of increasing titanium dioxide content on bulk and surface properties of phosphate-based glasses. *Acta Biomater* 2008; 4: 523–534.

15. Wall IB, Moseley R, Baird DM, et al. Fibroblast dysfunction is a key factor in the non-healing of chronic venous leg ulcers. *J Invest Dermatol* 2008; 128: 2526–2540.

16. Ahmadi R, Mordan N, Forbes A, et al. Enhanced attachment, growth and migration of smooth muscle cells on microcarriers produced using thermally induced phase separation. *Acta Biomater* 2011; 7: 1542–1549.

17. Lakhkar NJ, Lee IH, Kim HW, et al. Bone formation controlled by biologically relevant inorganic ions: Role and controlled delivery from phosphate-based glasses. *Adv Drug Deliv Rev* 2012. http://dx.doi.org/10.1016/j.addr.2012.05.015.

18. Yun YR, Jang JH, Jeon E, et al. Administration of growth factors for bone regeneration. *Regen Med* 2012; 7: 369–385.

19. Nichol JW and Khademhosseini A. Modular tissue engineering: engineering biological tissues from the bottom up. *Soft Matter* 2009; 5: 1312–1319.

20. Donos N, Retzepi M, Wall I, et al. *In vivo* gene expression profile of guided bone regeneration associated with a microrough titanium surface. *Clin Oral Implants Res* 2011; 22: 390–398.

21. Ivanovski S, Hamlet S, Retzepi M, et al. Transcriptional profiling of "guided bone regeneration" in a critical-size calvarial defect. *Clin Oral Implants Res* 2011; 22: 382–389.

22. Retzepi M, Lewis MP and Donos N. Effect of diabetes and metabolic control on de novo bone formation following guided bone regeneration. *Clin Oral Implants Res* 2010; 21: 71–79.

23. Senuma Y, Franceschin S, Hilborn JG, et al. Bioresorbable microspheres by spinning disk atomization as injectable cell carrier: from preparation to *in vitro* evaluation. *Biomaterials* 2000; 21: 1135–1144.